HISTRAP PROTOTYPE HARDWARE STUDIES*

D. K. Olsen, W. H. Atkins, D. T. Dowling, J. W. Johnson, R. S. Lord,**
J. W. McConnell, W. T. Milner, S. W. Mosko, and B. A. Tatum
Oak Ridge National Laboratory
Post Office Box 2008
Oak Ridge, Tennessee 37831-6368

ABSTRACT

HISTRAP, Heavy Ion Storage Ring for Atomic Physics, is a proposed 2.67-Tm synchrotron/ cooler/storage ring optimized for advanced atomic physics research which will be injected with ions from either the HHIRF 25-MV tandem accelerator or a dedicated ECR source and RFQ linac. Over the last two years, hardware prototypes have been developed for difficult and long lead-time components. A vacuum test stand, the rf cavity, and a prototype dipole magnet have been designed, constructed, and tested.

INTRODUCTION

HISTRAP is a proposed synchrotron/ cooler/ storage ring optimized to accelerate, decelerate, and store beams of highly-charged very-heavy ions at energies appropriate for advanced atomic physics research.[1] The ring is designed to allow studies of electron-ion, photon-ion, ion-atom, and ion-ion interactions. An electron cooling system will provide ion beams with small emittances and energy spread for precision spectroscopic studies and deceleration cycles. Figure 1 shows the proposed layout. The 46.8-m-circumference ring has a four-fold symmetry, with each quadrant consisting of a 4-m-long straight section and a 90° achromatic bending section. Each achromate consists of two 45° dipoles separated by a quadrupole triplet and sextupoles for chromatic correction. HISTRAP will be injected with ions from either the existing Holifield Heavy Ion Research Facility 25-MV tandem or from a dedicated 14.5-GHz ECR source and 250-keV/nucleon RFQ linac. The ring will have a bending power of between 0.1 and 2.67 Tm, and heavy ions will be stored with energies between 82 and 0.02 MeV/nucleon. A development program is under way in which prototypes of major HISTRAP components, including a vacuum test stand, an rf cavity, and a dipole magnet have been fabricated, assembled, and tested.

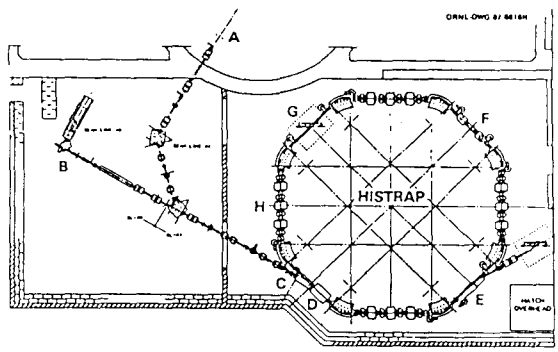

Fig. 1. Proposed HISTRAP facility. The ring has a circumference of 46.8 m, a maximum bending power of 2.67 Tm, and will be injected with either the HHIRF tandem or a dedicated ECR source and RFQ linac.

VACUUM TEST STAND

The 46.8-m circumference will be divided with eight gate valves so that each straight section, which requires 15-cm-diameter beam pipes, can be isolated. The bending sections require beam pipe with a similar cross section, giving a total ring vacuum chamber surface area in the order of 20 m^2. Heavy ions passing through residual gas in this chamber can either capture or lose electrons from

*Research sponsored by the U.S. Department of Energy under contract DE-AC05-84OR21400 with Martin Marietta Energy Systems, Inc.
**Consultant.

collisions with gas molecules. Estimates of beam lifetimes in HISTRAP from these charge-changing collisions were made using the electron capture cross sections of Schlacter[2] and electron loss cross sections of Alonso and Gould.[3] The vacuum requirement resulting from these calculations for a tandem injected and HISTRAP decelerated Au^{40+} beam, one of the worst possible vacuum cases, is severe. In particular, with a vacuum pressure of 3 x 10^{-12} Torr in a residual gas of 90% H_2 and 10% N_2, about 50% of a coasting 20 keV/nucleon Au^{40+} beam would be lost by electron capture in one second. Clearly, after deceleration of highly-charged very-heavy ions to low energies, HISTRAP storage times will be vacuum limited. Higher pressures are acceptable for acceleration cycles.

The vacuum test stand[4] shown in Fig. 2 was constructed to assess the problems associated with obtaining pressures in the 10^{-12} Torr region. This test stand approximately simulates 1/16 of the ring circumference and is a periodic system with a pump spacing of 1.75 m. The vacuum chamber

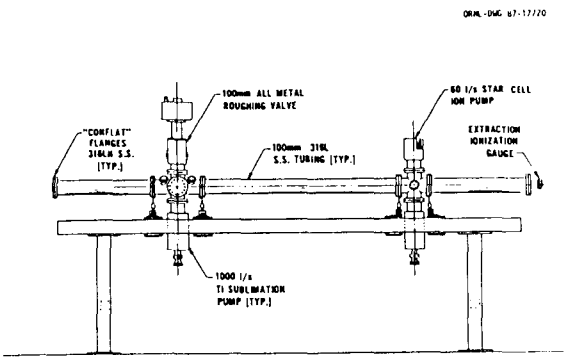

Fig. 2. UHV vacuum test stand which models 1/16th of the HISTRAP circumference. The stainless steel chambers were vacuum baked at 950°C prior to assembly and are covered with heater blankets for in situ bakes at 300°C.

components and sublimation pump housings were fabricated in-house from 316L and 316LN stainless steel 10-cm-diameter pipe and were prebaked at 950°C in a vacuum oven before final assembly. Pumping was accomplished by two 1000-ℓ/s titanium sublimation pumps (TSPs) and one 60-ℓ/s magnetic sputter ion pump (SIP). Heating blankets were used for in situ baking at temperatures up to 300°C. Pressures were measured with one Bayard-Alpert gauge, a residual gas analyzer (RGA), and extractor gauges at the minimum pressure position at the pump and maximum pressure position at the pipe end.

To eliminate all sources of oil contamination, the roughing system consisted of three stages of liquid-nitrogen-cooled sorption pumping, followed by an Air Products 20-cm-diameter closed-cycle gaseous helium cryopump. The cryopump was isolated from the sorption pumps and the main chamber by all-metal valves. The sorption pumps roughed the chamber and the cryopump to 3 x 10^{-3} Torr. After roughing to a pressure of 1 x 10^{-8} Torr with the cryopump, the chamber temperature was increased to 250°C at a rate of 30°C per hour. With only the cryopump, the system was baked for 48 hours and the pressure returned to 1 x 10^{-8} Torr.

During cool-down, the temperature was held fixed at 120°C with a pressure of 5 x 10^{-10} Torr while the TSPs, ion gauges, and RGA were degassed and the SIP was started. The titanium sublimators were each flashed for four minutes at 47 A and after the pressure recovered to 5 x 10^{-10} Torr, the all-metal valve to the cryopump was closed. The pump-down continued with the TSP and SIP, and after one week, minimum and maximum pressures of 3 x 10^{-12} and 7 x 10^{-12} Torr were achieved. The calculated outgassing rate of the stainless steel for this pressure was 3 x 10^{-13} Torr ℓ/cm^{-2}/S and an average pressure of 5 x 10^{-12} Torr was calculated for the equivalent periodic system.

The vacuum firing of the stainless steel at 950°C and the in situ 300°C bakeout produced residual outgassing rates which allowed reasonable pump sizes and spacing for obtaining pressures on the 10^{-12} Torr scale. The use of a cryopump for roughing during bakeout and cool-down provided contamination-free high-speed pumping.

HISTRAP RF CAVITY

In the standard high-current operating mode, heavy ions from the HHIRF tandem will be injected into HISTRAP with a magnetic rigidity of about 1.0 Tm with circulation frequencies between 1.0 MHz for $^{12}C^{6+}$ and 0.38 MHz for $^{238}U^{43+}$. These ions will be either accelerated to a maximum magnetic rigidity of 2.67 Tm with circulation frequencies between 2.7 MHz and 1.0 MHz, or decelerated to a minimum magnetic rigidity of 0.10 Tm with circulation frequencies between 0.10 MHz and 0.038 MHz. The longitudinal phase-space area of these injected beams will depend upon their mass, charge, energy/nucleon, and energy spread from post-tandem stripping foils. Most of the rf cavity voltage for HISTRAP is required to provide phase space area to accept these injected beams. For all ion species of interest from either injector, the maximum required peak accelerating voltage is 2.5 kV per turn. A tuning range between 0.2 MHz and 2.7 MHz is adequate using harmonic numbers between one and six. For operation with typical ions in the acceleration mode, the rf system should tune over most of the available frequency range within about 0.4 s.

A prototype rf cavity intended to meet these requirements has been designed, constructed, and tested. Estimated characteristics of the cavity are listed in Table 1. The cavity is a double quarter-wave, ferrite-loaded configuration with a single accelerating gap operated in the push-pull mode. Tuning is accomplished through varying a dc bias current in a set of "figure eight" bias windings. A photograph of the cavity is shown in Fig. 3. The center conductors of the cavity are mechanically separate from the high-vacuum beam line which contains the ceramic accelerating gap. Spring-loaded contact fingers, removable for baking, will provide electrical contact between the cavity electrodes and beam line.

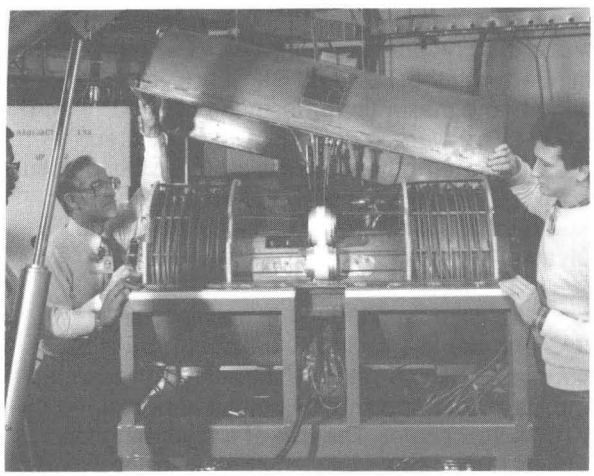

Fig. 3. Photograph of HISTRAP rf cavity.

The complete rf cavity will contain 28 ferrite rings, which are separated by 6.3-mm-thick water-cooled copper disks. The two ferrite-copper stacks are supported by fiberglass end plates which are joined by steel leadscrews. The prototype cavity has been only partially loaded with 16 ferrite rings, which is sufficient for testing and measuring the tuning and power dissipation characteristics. Approximately twice as much gap capacitance and rf drive power are required to operate the cavity with the test 16 rings than the design 28 rings.

Ferrite bias is provided through an array of three independent "figure eight" windings on each side of the gap. Outside bus connections are used for completing each "figure eight" winding so that the windings may be operated in series, parallel, or other arrangement, as needed to avoid rf parasitic modes. The prototype was operated with the three windings in series, and a 1000-A dc power supply was sufficient to swing the relative permeability over a 200 to 1 tuning range.

The ferrite rings were individually tested to measure relative permeability as a function of dc bias and rf excitation. Efforts to measure tuning characteristics of the individual rings were unsuccessful due to the intrinsic inductance in the test apparatus; however, tests with all 16 rings in the cavity were successful in demonstrating a tuning range from 0.25 to 3.0 MHz using a dc bias excitation up to 1000 A. The final tuning range of the complete cavity will be within the specified limits when the ferrite load is increased to 28 rings.

Test results are shown in Figs. 4 and 5. The low values of "Q" are especially interesting, since it will be possible to drive the cavity to frequencies substantially below resonance on the low end of the tuning range. This will provide some extension to the tuning range, and will provide needed tuner damping in the low-frequency region where small increments in ferrite bias cause a large change in resonant frequency. The shunt resistance of 80 ohms is nearly constant with frequency, so the cavity will operate comfortably with a balanced drive connected across the accelerating gap. The feasibility of operating an rf cavity with the tuning range required by HISTRAP has been demonstrated.

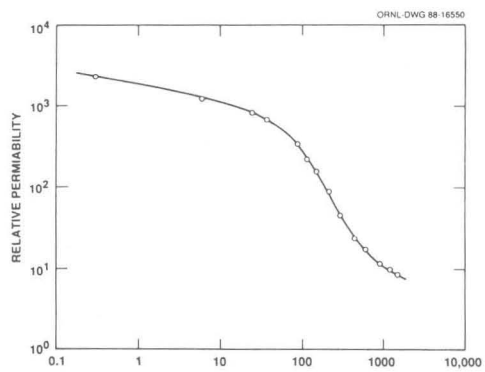

Fig. 4. Relative permeability of the TDK SY7 ferrite rings as a function of toroidal dc bias excitation.

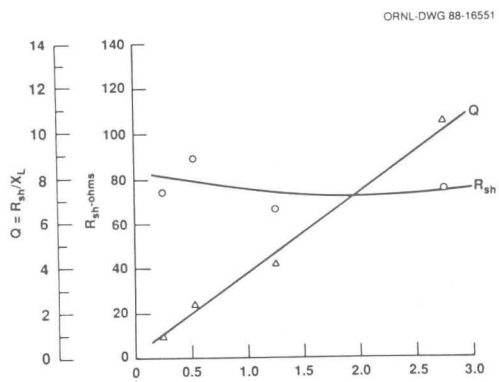

Fig. 5. Cavity "Q" and shunt resistance as a function of frequency.

PROTOTYPE DIPOLE MAGNET

The dipole magnets, the most important components in HISTRAP, present some special design problems. They are short with a large saggita, resulting in a complicated three-dimensional geometry and integrated field profiles which depend heavily on end effects. In addition, the dipoles have a large gap to provide space for vacuum bakeout insulation, have a "C" design to allow for merged laser beam studies, require a maximum field of 1.6 T, and need good field quality at both high and low excitation. To address these concerns, a prototype dipole has been designed, fabricated, and measured.

The dipole is a conventional laminated magnet with a 12.25 ton weight, a 123-cm-long yoke, a 12.8-cm sagitta, and parallel ends giving 22.5° beam entrance and exit angles. The laminations are 110 cm high, 101 cm wide, and the shims and Rogowski roll-off were essentially scaled from the FNAL designed and measured Loma Linda synchrotron dipoles.[7] Figure 6 shows calculated relative deviations from a pure dipole field as a function of horizontal distance from the central trajectory using the 3-D magnet code TOSCA. The upper curve of each type in Fig. 6 is the low-field result at 0.8 T and the corresponding lower curve is the high-field result at 1.6 T. The solid curves are the field profiles in the center of the dipole, excluding end effects, and are identical to those from the 2-D magnet code POISSON. The permeability drop at high field causes the two curves to separate by about 4 X 10^{-4} at ± 6 cm, the horizontal good-field width.

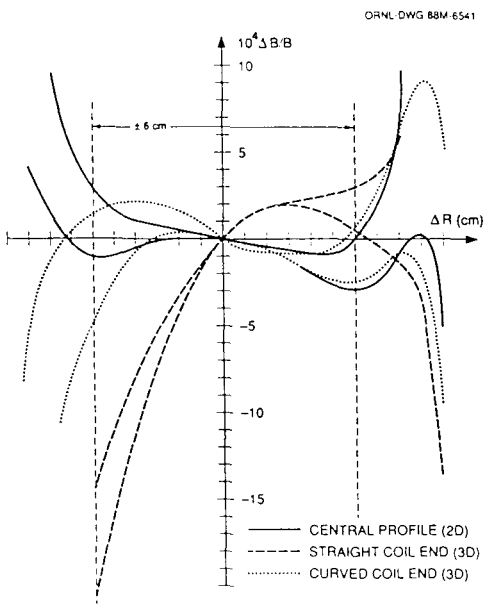

Fig. 6. 2-D and 3-D calculated field profiles for the HISTRAP prototype dipole magnet.

Equal inside and outside shims give a small quadrupole component to the field profile. The dashed and dotted curves show calculated 3-D TOSCA results, including end effects, obtained by integrating along the ion trajectories through the dipole. The dashed curves show the integrated profiles with straight coil ends parallel to the yoke end. The end effects are large and produce appreciable quadrupole and sextupole components. These components were significantly reduced by angling and curving the coil ends. These results are shown as the dotted curve. The end coil angle controls the quadrupole component and the end coil radius of curvature controls the sextupole component. The resultant coils are shown in Fig. 7.

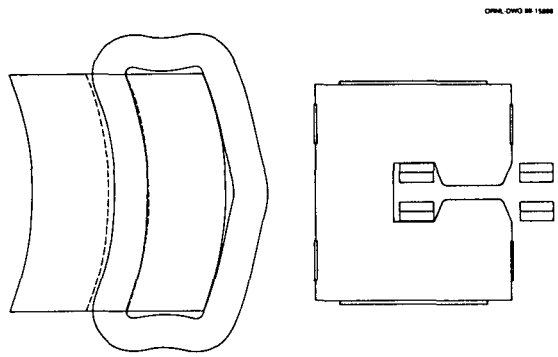

Fig. 7. HISTRAP prototype dipole magnet with a yoke length of 123 cm. The laminations are 101 cm x 110 cm.

Using this design, a prototype dipole was constructed by FNAL with laminations punched with a two-stage die from 16-gauge SAE 1004-1006 cold-rolled sheet steel purchased from Inland Steel. The steel was phosphate coated to provide electrical insulation between laminations and had a measured permeability of 182 at 100 Oersteds. The laminations were washed to improve adhesion, coated with a thin layer of epoxy, and then stacked in an assembly fixture. This fixture was used to stack both the yoke and end assemblies, which consist of removable 7.62-cm-thick end packs bolted to 2.54-cm-thick back packs which were machined with Rogowski contours. The laminations were stacked between these fabricated end assemblies with the gap facing down and centered about a vertical spacer projecting into the gap. Two rails determined the curvature of the magnet yoke. The yoke was then compressed to the proper length in the stacking fixture and fixed by welding 1.91-cm- thick steel plates to the top, bottom, and sides. Finally, the epoxy between laminations was cured at 300°C for five hours. The coil consists of four pancakes, each having 10 turns of 1.588-cm x 4.445-cm copper conductor. Electrical leads, water leads, and jumpers connect to the coils at the outside center of the dipole.

A mapping system using a temperature compensated Hall probe was built to measure the magnetic field of the dipoles and other magnetic elements. Positioning of the probe was accomplished by a personal computer (PC) based, x-y positioning system. Motion in both horizontal directions was obtained by mounting an aluminum bridge assembly on twin ball-bearing bushings which in turn were mounted on case-hardened and ground bearing shafts. Motion was controlled by driving a ball screw with stepping motors operated by a stepper-motor control board mounted in the PC. Step-to-pulse translator/driver/power supply units interface the PC board and motors. Optical linear scales of 0.01-mm resolution were mounted along each horizontal axis to provide position feedback via a digital readout box. An NMR probe was mounted in the dipole center for calibration checks of the Hall probe at regular intervals during mapping. Data were stored on a floppy disk.

The dipole midplane has been mapped at 15 excitation levels ranging from 72 to 2406 A, or 0.06 to 1.61 T. A map consists of 419 points along each of 21 curved orbits separated by 1 cm. Figure 8 shows representative middle and high field profiles. Each plot shows field profiles in the central region of the dipole (triangles) and profiles integrated along the ion path length (squares connected by lines). These measurements show a small quadrupole component in both the central and integrated profiles. This quadrupole component was not predicted by either TOSCA or POISSON and the origin of this difference is not understood. However, this quadrupole component can be compensated, if needed, by adjusting the main quadrupole strengths, fabricating pole face windings, or making small changes in the quadrupole spacings in the lattice. The measured sextupole and octupole components of the field are small and consistent withTOSCA predictions. With decreasing excitation, the quadrupole component decreases and changes sign. This decrease is consistent with a remnant field measurement of 30 G with a ± 2 G quadrupole component at ± 6 cm.

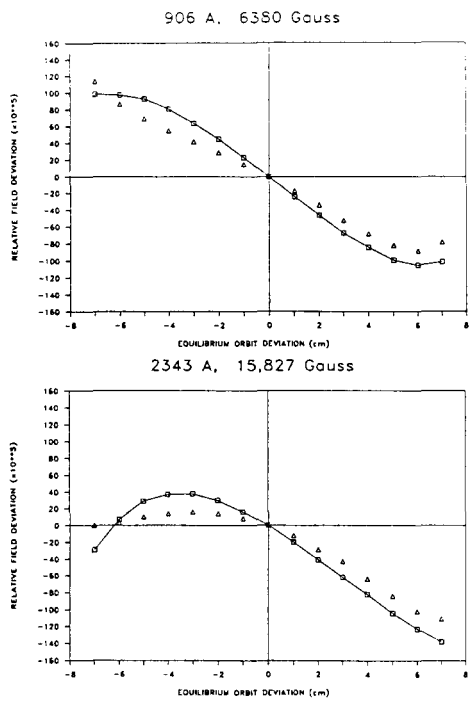

Fig. 8. Measured central (triangles) and path-length integrated (squares) field profiles in units of 10^{-5} as a function of orbit deviation.

The integrated profiles of each of the 15 mappings were least-squares fit for a polynomial of the form

$$\frac{B(x) - B_o}{B_o} = \frac{B'x}{B_o} + \frac{B''x^2}{2B_o} + \frac{B'''x^3}{6B_0}$$

where x is the equilibrium orbit deviation in meters. Table 2 gives the quadrupole, B'/B_o; sextupole, $B''/2B_o$; and octupole, $B'''/6B_o$ components integrated through the dipole. The magnet's effective ion path length is also tabulated.

REFERENCES

1. D. K. Olsen et al., Nucl. Instrum. and Meth. B24/25 (1987) 26.
2. A. S. Schlachter, Tenth International Conference on Cyclotrons and Their Applications, MSU, IEEE Catalog No. 84 CH1996-3, pp. 563.
3. J. Alonso and H. Gould, Phys. Rev. A26, 1134 (1982).
4. J. W. Johnson et al., American Vacuum Society 35th National Symposium and Topical Conf., Atlanta, October 1988.
5. S. W. Mosko et al., Proc. of 1989 Particle Accelerator Conference, Chicago, March 1989.
6. B. A. Tatum et al., Proc. of 1989 Particle Accelerator Conference, Chicago, March 1989.
7. F. Cole et al., Proc. of 1987 Particle Accelerator Conference, Washington, D.C., IEEE 87CH2387-9, 1985 (1987).

Table 1. RF Cavity Characteristics

Peak rf voltage	2500 volts
Tuning range	0.2 to 2.7 MHz
Overall length	1.2 meters
Beam tube diameter	0.15 meters
Center conductor OD	0.254 meters
Outer conductor ID	0.648 meters
Ferrite rings	
Material	TDK SY7 (NiZn)
ID	0.3 meters
OD	0.5 meters
Thickness	0.025 meters
Rings per cavity	28
Ferrite cooling	water cooled Cu separators
Peak power density in ferrite	200 mW/cc
Ferrite permeability range	8 to 1400
Peak ferrite bias current	3000 ampere turns
Shunt capacitance required	6000 pF
Total peak cavity rf drive power	20 kW

Table 2. Multipole Coefficients of the Dipole

Amp	Field Gauss	L-eff m	B'/B_o 1/m	$B''/2B_o$ $1/m^2$	$B'''/6B_o$ $1/m^3$
72	607	1.2793	0.0186	–0.0304	1.4241
125	863	1.2839	–0.0068	0.0284	1.3788
230	1587	1.2932	–0.0131	–0.0150	1.6267
327	2269	1.2967	–0.0224	–0.0160	1.8956
555	3887	1.2981	–0.0257	–0.0103	2.0764
704	4970	1.2983	–0.0241	–0.0126	1.8866
906	6380	1.2997	–0.0238	–0.0062	1.9210
1130	7959	1.2984	–0.0223	–0.0061	1.9090
1312	9249	1.2987	–0.0209	–0.0052	1.9218
1519	10650	1.2984	–0.0201	–0.0071	1.9669
1729	12181	1.2993	–0.0184	–0.0303	1.9597
1936	13537	1.2982	–0.0180	–0.0202	2.0052
2134	14800	1.2961	–0.0177	–0.0766	2.1099
2343	15827	1.2941	–0.0186	–0.1627	2.1994
2406	16111	1.2942	–0.0186	–0.1821	2.0858